J Mol Model (2003) 9:195–205
DOI 10.1007/s00894-002-0106-9

REVIEW

Pavla Čapková · Miroslav Pospíšil · Zdeněk Weiss

Combination of modeling and experiment in structure analysis of intercalated layer silicates

Received: 10 October 2002 / Accepted: 18 October 2002 / Published online: 16 April 2003

Abstract A strategy for the structure analysis of intercalated layer silicates based on a combination of modeling (i.e. force field calculations) and experiment is presented. Modeling in conjunction with experiment enables us to analyze the disordered intercalated structures of layer silicates where conventional diffraction analysis fails. Experiment plays a key role in the modeling strategy and in corroboration of the modeling results. X-ray powder diffraction and IR spectroscopy were found to be very useful complementary experiments to molecular modeling. Molecular mechanics and molecular dynamics simulations were carried out in the *Cerius*^{2} and *Materials Studio* modeling environments. An overview is given of the structures of layer silicates, especially smectites intercalated with various inorganic and organic guest species. Special attention is paid to the ordering of guests in the interlayer space, as it is important for the practical applications of these intercalates, where the interlayer porosity, photofunctions, etc. must be controlled.

Keywords Intercalated layer silicates · Structure analysis modeling · Molecular mechanics · Molecular dynamics

Introduction

Intercalation means an insertion of a guest molecule or ion into a suitable crystal structure without major rearrangement of the solid host structure. [1, 2, 3] Intercalation requires that the host structure has a strong covalent network of atoms, which remains unchanged on the intercalation reaction, and that there are vacant sites in the structure. These vacant sites should be interconnected and of suitable size to permit the diffusion of the guest species into the host structure. Layered crystal structures satisfy these requirements very well, being able to accommodate very large guest molecules in the interlayer space by the free adjustment of the interlayer separations.

Intercalated phyllosilicates are of great technological interest because of their applications in many fields of material research, industry and environmental issues. [4, 5, 6, 7, 8, 9, 10, 11, 12, 13, 14] Two different ways of intercalation can be used in the case of phyllosilicates: (1) ion-exchange reactions and (2) ion–dipole interactions. During intercalation based on ion-exchange reactions, the interlayer metal cations are exchanged with the organic or inorganic complex cations. Intercalation based on ion–dipole interactions means the adsorption of polar organic molecules such as alcohols, ketones, amides etc. interacting with interlayer cations and silicate layers. Smectites and vermiculite represent layer silicates, which are widely used as host structures for the intercalation of various organic and inorganic guest species.

Smectites belong to the group of 2:1 layer silicates with the disordered, so-called "turbostratic" layer stacking, characterized by the random shift and random azimuth rotation of two successive silicate layers. The structure of the 2:1 silicate layer (shown schematically in Fig. 1a, b) consists of one octahedral and two adjacent tetrahedral sheets. [15] Octahedra share octahedral edges. Tetrahedra in the tetrahedral sheet are linked, sharing three corners to form a hexagonal mesh pattern (Fig. 1a). The common plane of junction between the tetrahedral and octahedral sheets consists of the shared apical oxygens plus unshared OH groups that lie at the center of each tetrahedral six-fold ring at the same *z*-level as the apical oxygens. The smallest structural unit contains three octahedra. If all three octahedra are occupied, i.e. have octahedral cations at their centers, the silicate layer is classified as trioctahedral. If only two octahedra are occupied and the third octahedron is vacant, the layer is classified as dioctahedral. The octahedral cations are usually Mg, Al, Fe^{2+} and Fe^{3+}. The tetrahedral cations Si may be substituted for Al or Fe^{3+}. Substitutions of

P. Čapková (✉) · M. Pospíšil
Faculty of Mathematics and Physics,
Charles University Prague,
Ke Karlovu 3, 12116 Prague, Czech Republic
e-mail: capkova@karlov.mff.cuni.cz

Z. Weiss
Technical University Ostrava,
70833 Ostrava, Czech Republic

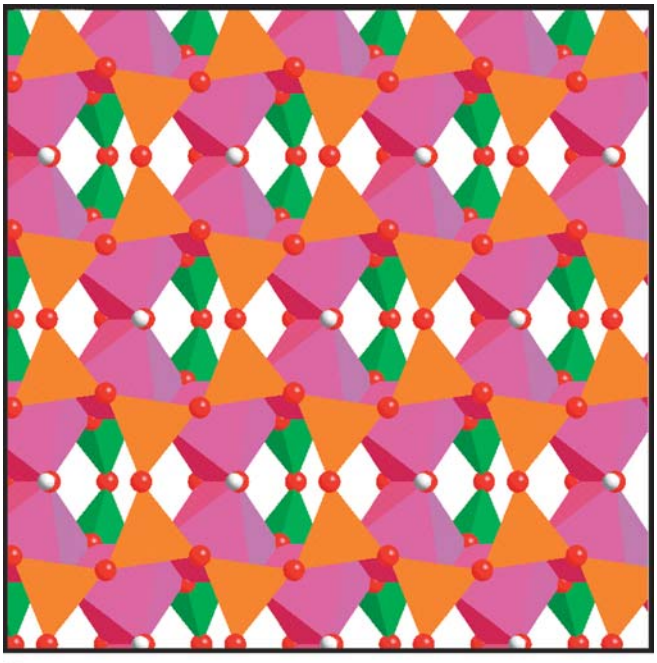

a

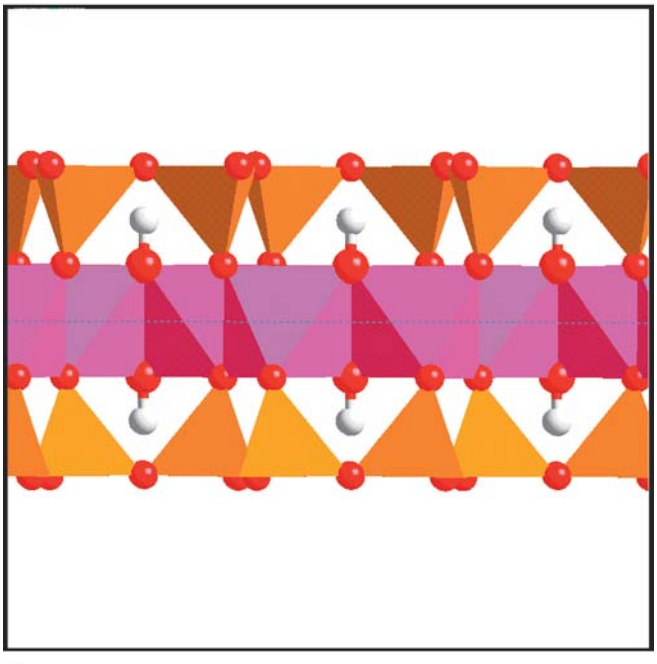

b

Fig. 1 **a** The top view of the silicate layer in dioctahedral 2:1 silicate, upper tetrahedral sheet (*yellow*) and lower tetrahedral sheet (*light green*). **b** The side view of the dioctahedral silicate layer

octahedral and tetrahedral cations for the cations with lower charge produce a resulting negative charge on the silicate layer, which is balanced by interlayer cations; these are commonly Na^{+}, Ca^{2+} and Mg^{2+}, but a wide range of inorganic and organic cations can be introduced by exchange reactions. Dioctahedral smectites with prevailing octahedral substitutions are called montmorillonites and analogically the trioctahedral smectites with prevailing octahedral substitutions are called hectorites. Dioctahedral smectites with prevailing tetrahedral substitutions are called beidellites and trioctahedral smectites with prevailing tetrahedral substitutions are called saponites.

Both substitutions, in octahedral as well as in tetrahedral sheets, create charge fluctuation in the surface oxygen layers and it is evident that the charge fluctuations caused by octahedral substitutions are lower. [16, 17] Consequently, no pronounced strong active sites in the host layer exist in montmorillonites and hectorites. As a result of this character of silicate layers, the arrangement of the guests and the layer stacking in intercalated montmorillonites and hectorites is disordered. [17, 18, 19] The irregularity in the positions of substituted atoms leads to an irregularity in the charge distribution in the surface oxygen layer, which is crucial for the anchoring of guest cations on the silicate layer. This irregular charge distribution leads to the irregular anchoring and arrangement of guests, even in the case of saponite and beidelite (smectites with prevailing tetrahedral substitutions), where the charge fluctuations in the surface oxygen layer are higher than in montmorillonite and hectorite. [16] Hence, the intercalation compounds of smectites display disordered guest structure and turbostratic disorder in layer stacking. [16, 17, 18, 19, 20]

Vermiculite belongs to the 2:1 trioctahedral phyllosilicates, but in contrast to saponite (i.e. trioctahedral smectite), the silicate layer in vermiculite has significantly higher layer charge. A priori, no qualitative distinction can be seen between the structural formulae of silicate layer for vermiculite and saponite: [21]

$$[Si_{8-x}Al_x]\left[Mg_{6-y}Al_y\right]O_{20}(OH)_4$$

where the values of x and y determine the layer charge per unit cell. According to [15], the formal charge per formula unit in saponite is approximately 1 el. unit, in vermiculite 1.2–1.8 el. units. Thanks to its relatively high layer charge, intercalated vermiculite exhibits two specific features in intercalation behavior:

- A stronger host–guest interaction in vermiculite than in saponite.
- A higher guest concentration in the interlayer space of vermiculite than in saponite. Consequently, guest–guest interactions become more important for the arrangement of guests in the interlayer space of vermiculite.

These conditions lead to the ordering of guests and consequently to the ordering of layers in intercalated vermiculite. The 3D order in the structure of intercalated vermiculite has been observed using single crystal diffraction data. [22, 23, 24]

The design of new intercalates with desired properties requires understanding the structure–property relationship. Hence, structure analysis plays a key role in research and technology of intercalates. However, the structural

disorder present in intercalated layer silicates seriously obstructs structure analysis based only on diffraction methods. Therefore, in the present work we pay attention to the method and strategy of structure analysis of intercalates using a combination of molecular modeling with experiment (diffraction methods and vibrational spectroscopy). Molecular mechanics and classical molecular dynamics simulations for structure analysis of intercalates were carried out in the *Cerius*^{2} and *Materials Studio* modeling environments (MSI/Accelrys). [25]

Strategy of structure analysis

The structure of intercalates is determined by the host–guest complementarity as well as other supramolecular systems. This can be characterized by the series of chemical and geometrical factors like the character of the active sites, the charge distribution on the host layers and guest species, topology of the host layers, the size of guests, etc. [26, 27, 28] These factors sometimes act in concert, leading to perfect structural ordering. The requirement of structural ordering is of great importance in the design of new intercalates for special applications, where one must control the interlayer porosity (selective sorbents, molecular sieves) or control the photofunctions of guest molecules in the interlayer space. Perfect three-dimensional order in intercalated structures requires perfect ordering of guest molecules in the interlayer space and consequently perfect order in the layer stacking. However, there is another factor that affects the structural order in intercalates. This is the rigidity of the guest molecules and the host layers. Intercalation of organic molecules containing long aliphatic chains may lead to chain distortions, depending on the chain length and on the guest concentration in the interlayer space. This effect will be illustrated in the next paragraph.

Intercalation is in fact an insertion of a known molecule into a known layered crystal structure. Consequently, structure analysis of layered intercalates must solve specific problems:

- To determine the positions, orientations and arrangement of the guest molecules in the interlayer space of the host structure
- To determine the possible changes in conformation of guest molecules due to the crystal field in the interlayer space of the host structure
- To determine the way of layer stacking in the intercalated structure
- To characterize a possible disorder in the intercalated structure

Intercalated layered structures very often exhibit various degrees of disorder in the positions and orientations of guest molecules and, thanks to the disorder, single crystals are not available for these materials. Powder diffraction patterns affected by the disorder are in addition influenced by the strong preferred orientation of crystallites [29] and by surface absorption due to the surface roughness effect. [30] Intercalation of organic guests into an inorganic host structure introduces an additional specific problem into the diffraction analysis of intercalates. X-ray scattering amplitudes of guest atoms, i.e. carbon, oxygen and hydrogen, are small in comparison with the atoms building the inorganic host structures and consequently the contribution of guest molecules to the total intensity diffracted from the crystal is too small. This complicates the localization of guests in the intercalated compounds from the diffraction data.

In such a case, molecular modeling is a very powerful tool in the structure analysis of intercalates, which is helpful especially in the correct interpretation of electron density maps obtained by X-ray diffraction data. However, it should be emphasized that modeling can provide reliable results only in conjunction with experiment. As convenient complementary experiments to molecular modeling, one can use X-ray and synchrotron diffraction, infrared spectroscopy and NMR spectroscopy, STM and AFM microscopy etc. Experiment plays an important role in creating the modeling strategy and in confirming modeling results. Complex structural analyses using a combination of modeling and experiment can provide us with a detailed structure model including characterization of the disorder. In addition to the diffraction analysis, we also obtain the total crystal energy, the sublimation energy, host–guest and guest–guest interaction energy and the charge distribution in the intercalated structure.

Modeling of intercalates

Molecular modeling (molecular mechanics) is a method of optimization of the structure and bonding geometry using minimization of the total potential energy of the crystal or molecular system. The energy of the system in molecular mechanics is described by an empirical force field. [25, 31] This simplified description of the crystal energy enables us to model large supramolecular systems that cannot be treated using ab initio calculations. The energy terms describing the valence interactions, i.e. bond stretching, angle bending, dihedral torsion and inversion, may differ in various force fields [25] and it is evident that the choice and testing of the force field belong to the most important parts of the modeling strategy. The force-field library in *Cerius*^{2} [25] contains the Universal Force Field [32] and several special force fields designed for modeling organic supramolecular systems, [33, 34] polymers, [35] and sorption of organic molecules into silicates and zeolites. [36] In the *Cerius*^{2} modeling environment, the atomic charges are calculated using the Qeq (Charge equilibration) method, [37] and the Ewald summation method [38, 39] is used to calculate the Coulomb energy. Lennard-Jones potentials are used for calculating van der Waals interactions.

Classical molecular dynamics calculates the dynamic trajectory of the system by solving the classical equations of motion for a system of interacting atoms. [25, 31] The

temperature and distribution of atomic velocities in the system are related through the Maxwell–Boltzmann equation. Introducing temperature and pressure control into molecular dynamics enables us to study temperature-dependent processes and to explore the local conformational space. However, for crossing large energy barriers, molecular dynamics at high temperatures can be used.

All computational methods that search for the global energy minimum must generate a large number of initial models using one of three different ways: [31, 40]

1. A deterministic method for generating starting models, performing a systematic grid search that covers all areas of the potential energy surface [40, 41, 42]
2. Molecular dynamics generating the starting geometry [25, 31, 43]
3. Stochastic methods (Monte Carlo, [43] Genetic Algorithm, ... [44])

The first method, performing a systematic grid search, can be used easily to generate starting models in the case of small or rigid large guests and rigid host layers. On the other hand molecular dynamics is very well suited for generating starting models in the case of large flexible organic guest molecules. For modeling layer silicates intercalated with organic guests we used molecular dynamics in *Cerius*^{2}. The strategy of modeling consists of building initial models, setting up the energy expression, the choice and testing of the force field, definition of rigid fragments and setting up fixed and variable structure parameters etc. Reliable results of modeling can be obtained providing that all the steps in the modeling strategy are based on available experimental data.

Diffraction data in the modeling strategy

Although the powder diffraction data may be affected by structural disorder and sample effects like the preferred orientation of crystallites and eventual surface roughness, it can always provide us with some information that is useful for the strategy of modeling. At the least, we can obtain the basal spacing (interlayer distance) and an indication of the type of the disorder. In more favorable cases, we can even obtain the lattice parameters of the intercalated structure. These experimental data are valuable in building the initial model for the energy minimization. By comparing the diffraction pattern for the intercalated and host structures, one can deduce the changes of structural parameters after intercalation and, consequently, set up the most suitable modeling strategy (i.e. the variable and fixed structure parameters, rigidity of the host layers etc.).

Comparison of diffraction line profiles of the host structure and intercalate provide us with information about the character and degree of disorder, which may appear in the intercalated structure. Disorder in the arrangement of guests in the interlayer space leads to lattice strain accompanied by fluctuations in the basal spacing and to disorder in the layer stacking. Both effects (basal spacing fluctuation and disorder in the layer stacking) exhibit characteristic broadening of diffraction profiles. This information is very helpful for the modeling strategy and for the interpretation of the modeling results.

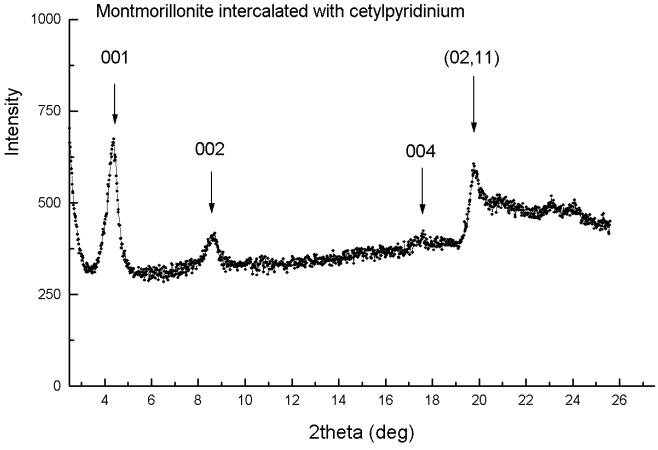

Fig. 2 X-ray powder diffraction diagram of montmorillonite intercalated with cetylpyridinium

Let us illustrate the use of diffraction data in the modeling strategy for montmorillonite intercalated with cetylpyridinium cations. [45] Figure 2 shows the X-ray powder diffraction pattern of montmorillonite intercalated with cetylpyridinium. The strong basal reflections 00*l* show the basal spacing of the intercalated structure to be 20.59 Å. The line broadening of the 00*l* reflections indicates the disorder in the interlayer structure (the full width at half maximum for reflection profile 002 is ~0.60° on the 2θ scale). The position and profile of the *hk* band (02,11) at 2θ=19.80° indicates that turbostratic layer stacking and the characteristic *a,b* lattice parameters remain the same in intercalated and host structures. The presence of *hk* bands in both structures indicates turbostratic disorder in the host structure and intercalate. The same position of *hk* bands in the host structure and the intercalate shows that the lattice parameters *a*, *b* of the silicate layer remain the same in the intercalate as in the host structure. This means that the structure of the silicate layers is not affected by the intercalation, i.e. the silicate layers behave as rigid bodies during intercalation. This conclusion is very important for the modeling strategy.

IR spectra in modeling strategy

Comparing the three IR spectra of (1) the intercalate, (2) the pristine guest compound and (3) the host compound, we can see possible changes in the bonding geometry and conformation of guest molecules and host layers, which may occur during the intercalation. If the spectral bands corresponding to the host layers exhibit the same positions and profiles in the host structure and intercalate, one can conclude that there are no changes in bonding

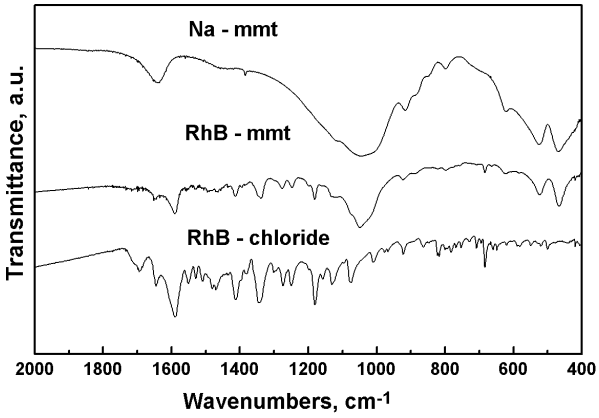

Fig. 3 Comparison of the IR spectra of the host structure Na-montmorillonite (Na-mmt) and the spectrum of the pristine guest compound rhodamine B chloride (RhB-chloride) with the spectrum of the intercalate rhodamine B^+–montmorillonite (RHB-mmt)

geometry of the host layers during intercalation. The rigidity of the host layers is very important for the modeling strategy, as in such a case the host layers can be treated as rigid units during energy minimization. The same conclusion can be derived for the guest molecules. The rigidity of the host layers is the crucial assumption in the modeling of intercalates, as in this case force field calculations of bonding geometry are not feasible.

Figure 3 shows a comparison of IR spectra for the host structure Na-montmorillonite, rhodamine B–montmorillonite and guest compound rhodamine B chloride. As one can see, the IR spectrum for the intercalate includes all bands characteristic for the silicate layer and also the bands characteristic for the rhodamine B. This comparison supports the rigidity of the silicate layers and suggests also only small changes in the bonding geometry of rhodamine B. (A detailed description is given in the next section.)

Smectites intercalated with inorganic complex cations

Various inorganic complex cations have been used as guests for intercalation in smectites to design new sorbents and catalysts. The goal in this case is to prepare nanoporous structures, called "pillared clays", where the large inorganic cations are intercalated in the interlayer space. The most frequently used pillars are complex cations with aluminum, [17, 18] chromium, [46] iron [47] and zirconium. [48] However, the main problem in pillaring clays is the host–guest complementarity. The structure of the inorganic complex cations used does not exhibit perfect geometrical complementarity to the structure of the silicate layer. Consequently, the anchoring of these guests to the host layers is not regular in smectites. [18]

This disorder in the arrangement of the guests has unfavorable consequences for all practical applications

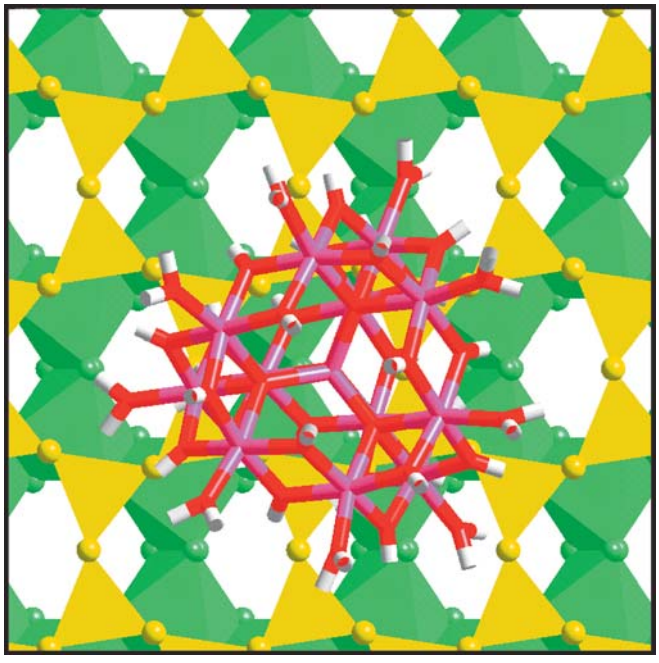

Fig. 4 Keggin cation $[Al_{13}O4(OH)_{24}(H_2O)_{12}]^{7+}$ attached to the silicate layer in the interlayer space of montmorillonite. For clarity only octahedral and upper tetrahedral sheets are visualized. The top view illustrates the geometrical host–guest incomplementarity

where the interlayer porosity should be under control. This is also the key enduring problem in the development of selective sorbents based on clays intercalated with large complex cations. Figure 4 shows the Keggin cation $[Al_{13}O4(OH)_{24}(H_2O)_{12}]^{7+}$ attached to the montmorillonite layer. This cation has been used widely as the pillar in smectite host structures [10, 11, 12, 13, 14, 19] and, as one can see in Fig. 4, in addition to the absence of strong pronounced active sites on the montmorillonite layer, there is no geometrical host–guest complementarity. Moving the cation along the host layer in any direction, one obtains only small changes in the host–guest interaction and total crystal energy. Consequently, no preferential positions exist for anchoring the guests. [18] This result of modeling [18] is in agreement with the results of X-ray diffraction analysis.

Organically modified clays

On the other hand, smectites can be used as a convenient host matrix for intercalates where the ordering of guest structure is not important for the desired properties. For example, an intercalation of various cationic surfactants must create precursors with a hydrophobic interlayer [8, 49, 50] for further intercalation of organic molecules or oligomers to prepare sorbents, [51] catalysts, [9, 52] polymer–clay nanocomposites [53] etc. The present search for new materials based on organically modified clays is focused on three main fields:

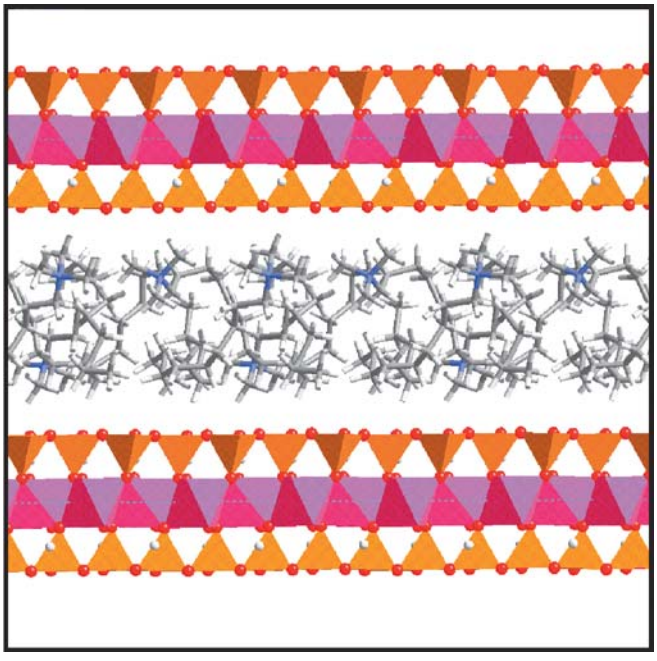

Fig. 5 Liquid-like arrangement of guest structure in montmorillonite intercalated with cetyltrimethylammonium

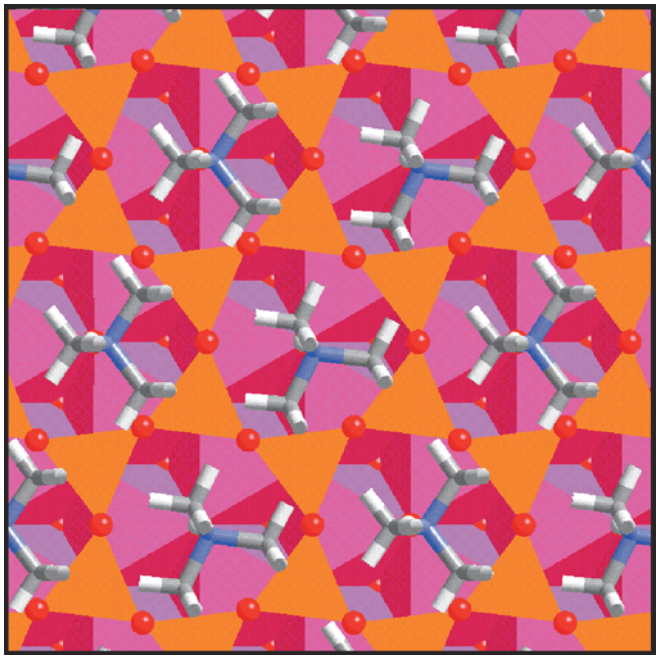

Fig. 6 Ordered structure of vermiculite intercalated with tetramethylammonium. Top view shows the anchoring of the TMA cations to the trioctahedral silicate layer

- Development of a new sorbents and catalysts [49, 50, 51, 52]
- Development of new supramolecular systems with optically active molecules attached to silicate layers exhibiting new or improved photofunctions [4, 8, 54]
- Development of a new polymer–clay nanocomposites [53, 55]

Intercalation with organoammonium cations

Organoammonium cations (especially alkylammonium) belong to the widely used surfactants on the silicate layers. They promote the sorption of neutral organic molecules due to the hydrophobic effect. Consequently, surfactants enhance the sorptive capacities of clays for organic contaminants [56, 57, 58, 59] and enable the subsequent intercalation of polar organic molecules for various purposes (polymer–clay nanocomposites, photofunctional systems).

The interlayer structure of smectites intercalated with alkylammonium cations is a result of an interplay of several factors: the density of the layer charge, the degree of exchange, [60] the length of the alkyl chain, [61] and the host–guest and guest–guest interaction energies. The structures of clays with cationic surfactants are disordered thanks to the flexibility of these organic cations and due to their irregular anchoring to the silicate layers. [45] Figure 5 shows the liquid-like arrangement of cetyltrimethylammonium cations in the interlayer space of montmorillonite, which is typical for this type of structure. This structure was calculated using molecular dynamics simulations in *Cerius*^{2} [45] and the calculated basal spacing of 18.10 Å was in good agreement with the experimental value, 18.00 Å. The same character of structure was found for montmorillonite intercalated with cetylpyridinium. [45]

Modeling of vermiculite intercalated with tetramethyammonium (TMA) and anilinium [62] carried out in *Cerius*^{2} led to ordered intercalated structures, which have been observed by X-ray single crystal diffraction. [22] This structure ordering in vermiculite is the result of the high layer charge and consequently the high concentration of guests compensating the high layer charge. In this case, the stronger interactions between guests in the interlayer space are among the important factors ruling the interlayer guest structure. Let us compare the structure of vermiculite and montmorillonite intercalated with tetramethylammonium. Figure 6 shows the ordered structure of TMA–vermiculite, while the disordered structure of TMA–montmorillonite is in Fig. 7 (the same disorder can be observed in all smectites). While in montmorillonite with low layer charge and low guest concentration the main interaction ruling the crystal packing is the host–guest interaction, in vermiculite the ordered structure is the result of competition between the host–guest and guest–guest interactions.

Charge analysis revealed the differences in the intercalation behaviors of montmorillonite, beidelite and vermiculite. [16, 63] Partial charges calculated in *Cerius*^{2} and summarized in the Table 1 are related to one supercell $2a \times 2b \times 1c$. As one can see in Table 1, the host–guest charge polarization increases on going from TMA–montmorillonite via TMA–beidelite to TMA–vermiculite

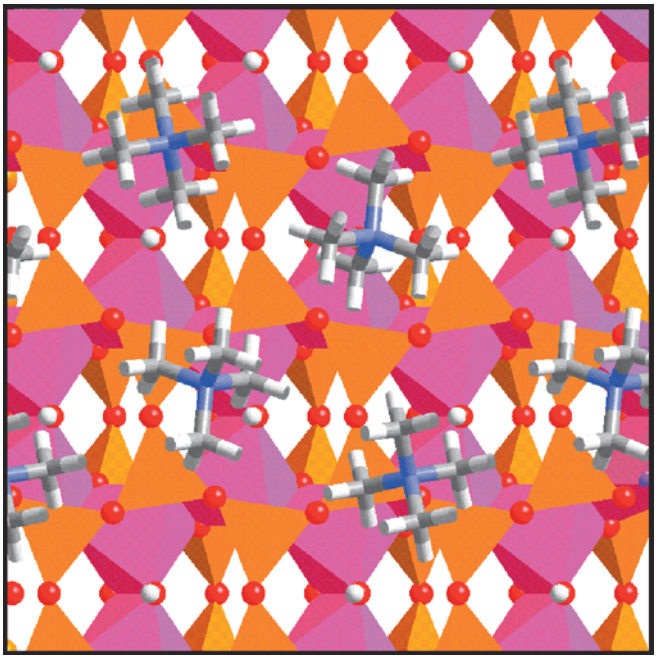

Fig. 7 Disordered structure of montmorillonite (dioctahedral silicate layer) intercalated with tetramethylammonium cations

(compare the total layer charge and charges on the TMA cations). Charge fluctuations on the surface oxygen sheet exhibit the same tendency, as is evident from comparison of the intervals of the oxygen charges for TMA–montmorillonite, –beidellite and –vermiculite (first line of Table 1).

Intercalation with rhodamine B

The intercalation of xanthene dyes in smectite-type clays is followed by the changes observed in the absorption spectrum (the so-called metachromatic effect), whereby the main absorption band is shifted to higher energies. [64, 65, 66] This effect is explained by (i) the interaction between the aluminosilicate layers and the dye (i.e. the interaction between the electron lone pairs of clay surface oxygens and the dye π system) and (ii) the interaction between the dye molecules in the interlayer space of the clay structure (i.e. dimerization and the π–π interaction between two monomers in the dimer). Rhodamine dyes are considered good probe molecules for studying clay–dye complexes, as they can easily be intercalated into the clay structure via a cation-exchange mechanism and their photophysics depends on the environmental factors.

The structure of montmorillonite intercalated with rhodamine B was investigated using a combination of powder diffraction and molecular modeling in *Cerius*^{2}. [63] The molecular mechanics and dynamics simulations result in two types of interlayer structure with basal spacings of 18.1 Å (phase 18 Å) and ~23 Å (phase 23 Å). The existence of these two phases was corroborated by experiment (X-ray powder diffraction). The two phases differ significantly in the interlayer structure, but they exhibit certain common features. First of all, no regular ordered positions for the rhodamine B anchoring to the silicate layers were found, neither for phase 18 Å nor for 23 Å. Intramolecular rotation about the xanthene–amine bonds has been observed in both phases. The carboxyphenyl rings may rotate about the xanthene–phenyl bonds in both phases and in all arrangements of rhodamine B cations. The carboxyl groups can rotate about the phenyl–carboxyl (C–C) bonds. The slight distortion of the planar xanthene part of the rhodamine B cation has been observed in both phases 18 Å and 23 Å and confirmed by IR spectroscopy.

In the phase 18 Å (d_{001}=18.1 Å), the arrangement of rhodamine B cations is bilayer. In both guest layers the long axis of the xanthene ring along the N–N line is nearly parallel with the silicate layers. The phase 18 Å exhibits two types of interlayer structures with the same basal spacing and nearly the same total sublimation energy:

1. Dimeric-sandwich type, called H-dimers in the literature [67, 68] (see Fig. 8a, b). In H-dimers the rhodamine B cations interact with each other via the carboxyl groups. A detailed view of the H-dimer is shown in Fig. 8b. One can see the carboxyl groups pointed to the oxygen atom in the xanthene ring of the neighboring rhodamine B cation. It is also evident from Fig. 8b that the double xanthene=amine bonds of the two cations in the dimer are oriented in the same direction (head-to-head arrangement). The total sublimation energy per one supercell of montmorillonite $3a\times2b\times1c$ is 876 kcal mol^{-1}.
2. The monomeric bilayer arrangement is shown in Fig. 9, which shows the top view of the interlayer arrange-

Table 1 Total charges per supercell calculated on the silicate layer for the individual sheets of atomic planes in electron units. *Q*-silicate layer is the total charge on the silicate layer per $2a\times2b\times1c$ supercell and *Q*-TMA is the total charge on one TMA cation

Charges (el. units)	TMA–MMT	TMA–BEID	TMA–VER
Charge fluctuation on the surface oxygen atoms	−0.63–(−0.66)	−0.61–(−0.66)	−0.63–(−0.70)
Q-oxygen (surface)	−15.335	−15.382	−16.104
Q-Si/Al (tetr. cations)	+20.648	+20.216	+19.331
Q-H	+1.758	+1.775	+1.369
Q-oxygen (apical+O_H)	−16.052	−16.602	−15.109
Q-Al/Mg (oct. cation)	+17.77	+19.316	+19.030
Q-silicate layer (total)	−0.200	−0.668	−1.955
Q-TMA cation	+0.050	+0.167	+0.244

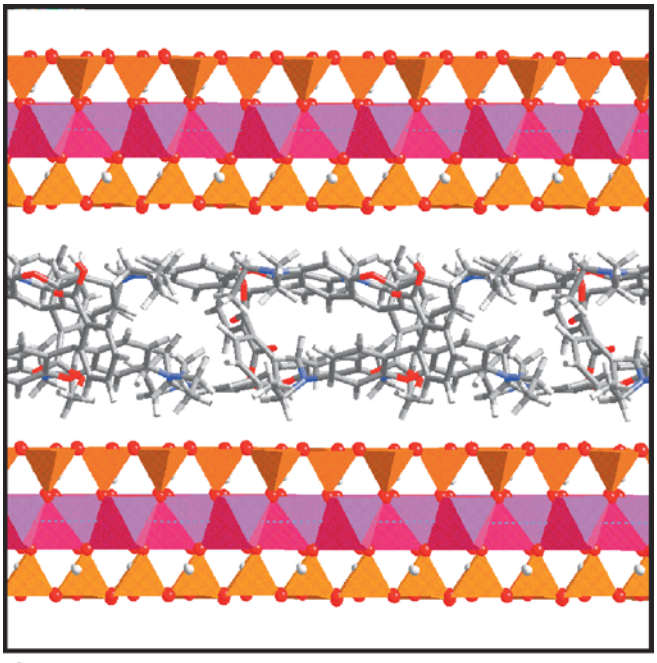

a

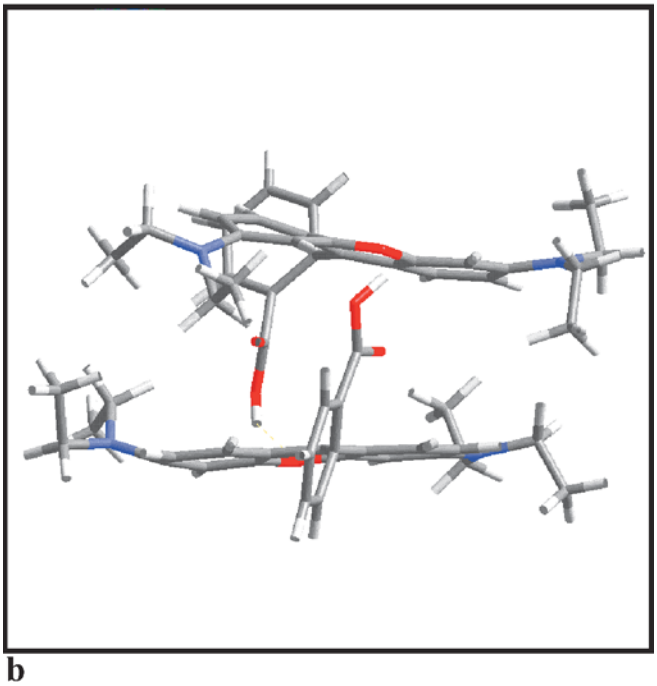

b

Fig. 8 **a** Dimeric sandwich-type of bilayer arrangement (H-dimers) of the rhodamine B cations in the interlayer space of montmorillonite in the phase 18 Å. **b** Detailed view of the H-dimer

ment of the rhodamine B guests, where only weak interactions between the guest were detected. The basal spacing for this model is the same as for the H-dimeric structure, 18.1 Å. The total sublimation energy is 842 kcal mol^{-1}.

Inclusion of the water molecules into the interlayer space of the phase 18 Å leads to a significant increase in the total sublimation energy. This means the sorption of water to stabilize the structure is very probable. This conclusion of modeling agrees with experimental observations.

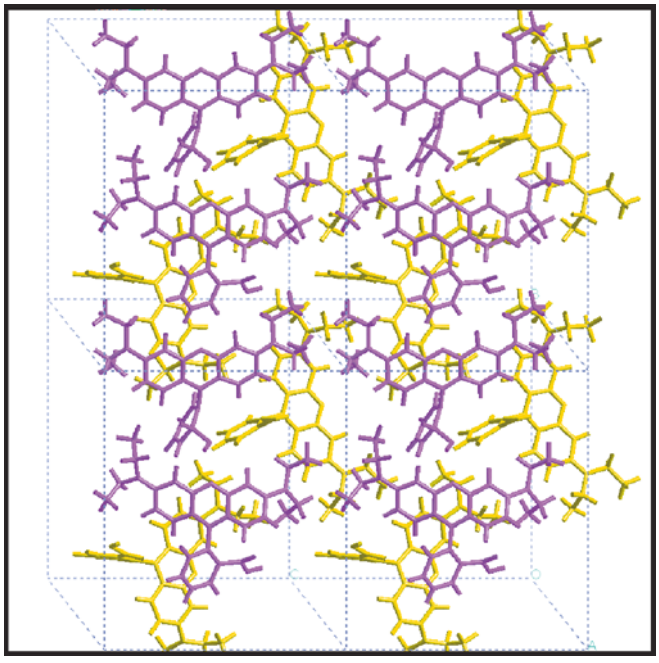

Fig. 9 Upper and lower layer in the monomeric bilayer arrangement of rhodamine B cations intercalated in montmorillonite (the phase 18 Å)

The phase 23 Å was observed using an intercalation solution with a very low concentration of guests with a prevailing monomeric arrangement. The modeling of the monomeric arrangement in the interlayer space of montmorillonite led to: (i) the bilayer arrangement (phase 18 Å) described above and (ii) to the monolayer arrangement of tilted monomers with basal spacing within 21–25 Å, which we have denoted as "phase 23 Å". An example of this structure is shown in Fig. 10. In this phase 23 Å, the rhodamine B cations are tilted relative to the silicate layers. The tilt angles are in the range 40–60°. This wide range of positions and orientations of the rhodamine B cations in the interlayer results in disorder and strain in the interlayer space, which is additionally intensified by the presence of interlayer water and leads to the large fluctuations of the basal spacing. In the phase 23 Å, a mixture of monomers and dimers was found in the interlamellar space. Two types of head-to-tail dimers found in this structure are illustrated in Fig. 11a and b. The dimer shown in Fig. 11a is the head-to-tail sandwich type (note the position of the single and double xanthene–amine bonds!). On the other hand, the head-to-tail dimer in Fig. 11b is the so-called J-dimer, which has been described in the literature. [67, 68] It is evident that the J-dimer allows a higher degree of aggregation in the interlamellar space of montmorillonite. Insertion of water molecules into the interlayer structure of the phase 23 Å

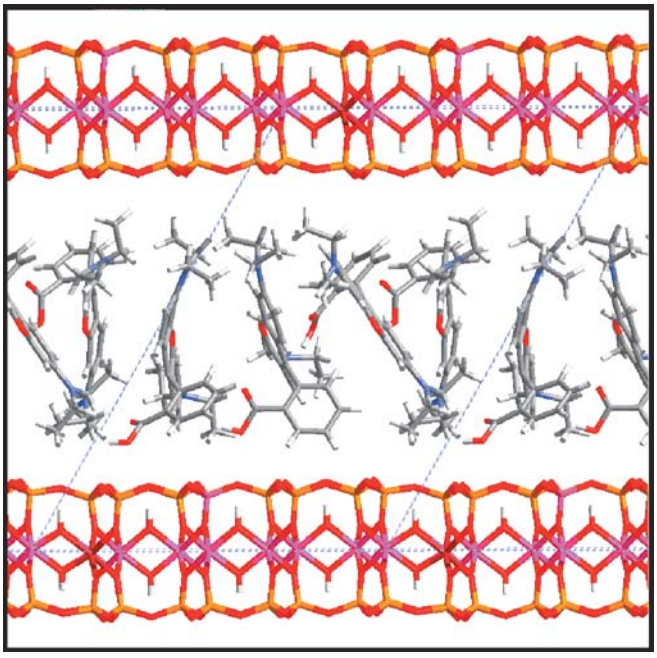

Fig. 10 Monolayer arrangement of [rhodamine B]$^+$ in the phase 23 Å. A mixture of monomers and dimers was found in this interlayer guest structure

leads to fluctuations of the basal spacing within the range 21–25 Å.

Intercalation based on ion–dipole interaction

Many organic molecules with polar functional groups can be intercalated in the interlayer space of montmorillonite, producing swelling. If the neutral molecules of alkylamines are intercalated in Na-montmorillonite, the Na^+ cations remain in the interlayer space and the structure of the interlayer depends on the concentration of guest molecules, on the host–guest and guest–guest interaction and in addition on the ion–dipole interaction between the guest molecules and Na^+ cations. However, in case of the ion exchange intercalation reaction the guest concentration in the interlayer space is ruled by the silicate layer charge (see Fig. 5), and the neutral molecules of alkylamine can enter into the interlayer space in high concentration, arranged in monolayer or bilayer arrangements. [69]

The effect of guest concentration on the interlayer structure will be illustrated using the example of Na^+-montmorillonite intercalated with octadecylamine (ODAMIN). The intercalation reaction in this case is based on the ion–dipole interaction; i.e. Na^+ cations remain present in the interlayer space. The aim of this study is to prepare an intercalate useful as a precursor for subsequent intercalation of further polar organic molecules with a low energy of exfoliation for potential use in polymer/clay nanocomposites technology.

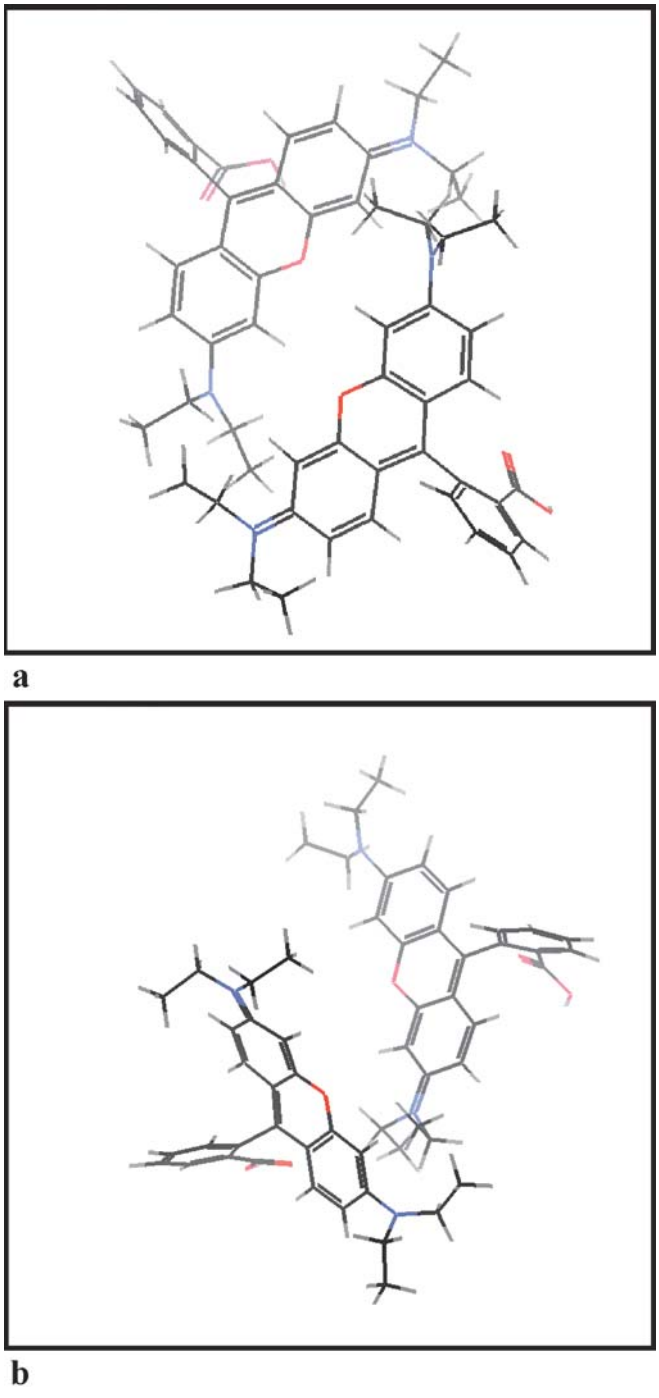

Fig. 11 **a** Detailed view of the head-to-tail sandwich type of dimer observed in the phase 23 Å (monolayer arrangement of rhodamine B cations). **b** Head-to-tail J-dimer observed in the phase 23 Å

Molecular mechanics and molecular dynamics simulations showed that the arrangement of guests in ODAMIN–montmorillonite can be monolayer or bilayer, depending on the ODAMIN concentration. These two phases with monolayer and bilayer guest structure were found by modeling and observed by X-ray powder diffraction. Structures are shown in Figs. 12 and 13, where one can see that the alkyl chains are ordered in

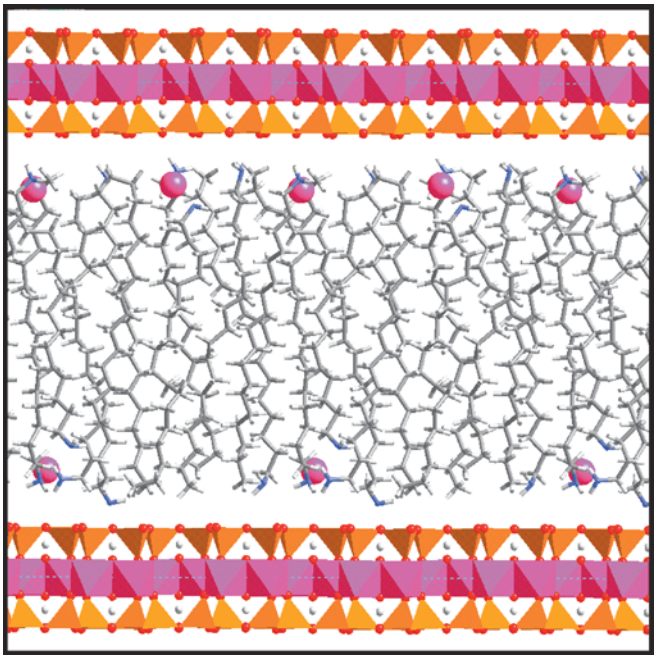

Fig. 12 Structure of montmorillonite intercalated with octadecylamine via ion–dipole interaction with maximum concentration of guests corresponding to the monolayer arrangement of guests with basal spacing 33.3 Å. The Na cations remaining in the interlayer are visualized as *pink* balls

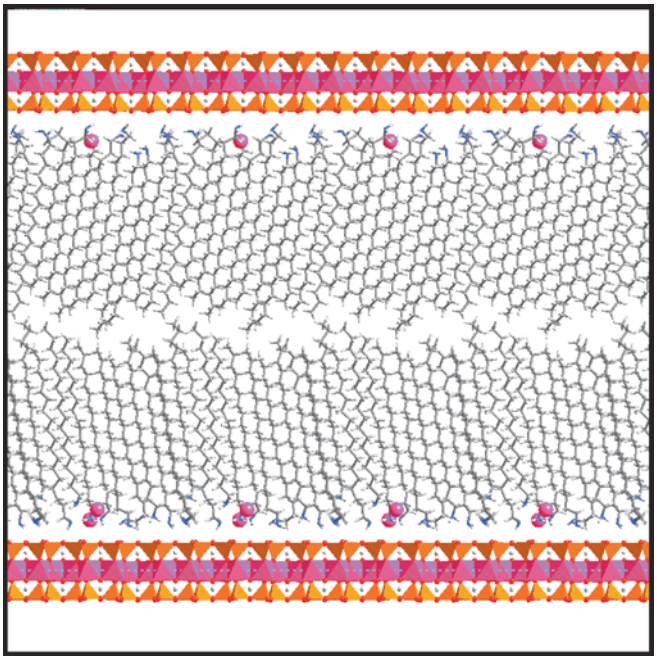

Fig. 13 Structure of montmorillonite intercalated with octadecylamine with maximum concentration of guests corresponding to the bilayer arrangement of guests with basal spacing 58.0 Å

comparison with the liquid-like arrangements of cetyltrimethylammonium cations in Fig. 5. Modeling and X-ray diffraction also confirmed that a series of intermediate phases can exist, such as a disordered monolayer with low ODAMIN concentration or two disordered overlapping ODAMIN layers. The calculated basal spacing for the pure phase with monolayer guests is 33.3 Å (see Fig. 12), while the measured value is 32.6 Å. For the bilayer arrangement of guests the calculated basal spacing of 58.6 Å was in good agreement with the experimental value of 58.0 Å.

The significant difference between these two phases was found in the values of the exfoliation energy related to one $2a \times 2b \times 1c$ supercell of montmorillonite. This parameter is important for polymer–clay nanocomposite technology and characterizes the energy necessary for breaking the interlayer bonding in the intercalated structure. For the monolayer arrangement of guests, the exfoliation energy was found to be 144.7 kcal mol^{-1} and for the bilayer arrangement 37.6 kcal mol^{-1}.

Conclusions

Intercalation is a very promising route to synthesis of new materials with desired properties, which can be tuned by the proper choice of host–guest combination, by the guest concentration and by co-intercalation of further guest species. This field represents a challenge for molecular modeling. Molecular mechanics and classical molecular dynamics (using empirical force fields) can provide us with a fast analysis of the host–guest complementarity and hence with a search for the most suitable host–guest combination for a given purpose. Modeling is a valuable tool in the structure analysis of intercalated layer silicates with disordered structures, where pure diffraction analysis is not feasible. In addition to the structure model, we can perform analyses of charges and interaction energies. These characteristics are very helpful in the design of supramolecular systems. It should be emphasized that a combination of modeling with experiment is necessary for a reasonable use of modeling that leads to reliable results.

Acknowledgements This work was supported by the grant agency GAČR grant no: 205/02/0941 and the grant agency of the Ministry of education FRVŠ grant no: 2408/2002.

References

1. Jacobson AJ (1992) Intercalation reaction of layered compounds, chapter 6. In: Cheetham AK, Day P (eds) Solid state chemistry compounds. Clarendon Press, Oxford, pp 182–200
2. Schölhorn R (1984) In: Atwood JL, Davies JED, MacNicol DD (eds) Inclusion compounds. Academic Press, New York, pp 249–349
3. Lerf A (2000) Intercalation compounds in layered host lattices: supramolecular chemistry in nanodimensions. In: Nalwa HS (ed) Handbook of nanostructured materials and nanotechnology, vol 5. Academic Press, New York, pp 1–166
4. Ogawa M, Kuroda K (1995) Chem Rev 95:399–438

5. Lagaly G (1986) Solid State Ionics 22:43–51
6. Clearfield A (1982) Inorganic ion exchange material. In: Clearfield A (ed) Inorganic ion exchange material. CRC Press, Boca Raton, Fla., pp 3–115
7. Alberti G (1987) In: Williams PA, Hudson MJ (eds) Recent developments in ion exchange. Elsevier, London, pp 233–248
8. Ogawa M, Aono T, Kuroda K, Kato C (1993) Langmuir 9:1529–1533
9. Galarneau A, Barodawalla A, Pinnavaia TJ (1997) Chem Commun 17:1661–1662
10. Pinnavaia TJ, Tzou MS, Landau SD, Raythatha RH (1984) J Mol Catal 27:195–212
11. Schoonheydt RA, Leeman H, Scorpion A, Lenotte I, Grobet P (1994) Clay Clay Miner 42:518–525
12. Figueras F, Klapyta Z, Massiani P, Mountassir Z, Tichit D, Fajula F, Gueguen C, Bousquet J, Auroux A (1990) Clay Clay Miner 38:257–264
13. Malla PB, Komarneni S (1993) Clay Clay Miner 41:472–483
14. Zhao D, Wang G, Yang Y, Guo X, Wang Q, Ren J (1993) Clay Clay Miner 41:317–327
15. Brindley GW (1980) In: Brindley GW, Brown G (eds) Crystal structures of clay minerals and their X-ray identification. Mineralogical Society, Monograph No 5, London, pp 125–197
16. Čapková P, Pospíšil M, Miehé-Brendlé J, Trchová M, Weiss Z, Le Dred R (2000) J Mol Model 6:600–607
17. Pruissen DJ, Čapková P, Driessen RAJ, Schenk H (2000) App Catal A General 193:103–112
18. Čapková P, Driessen RAJ, Schenk H, Weiss Z (1997) J Mol Model 3:467–472
19. Čapková P, Driessen RAJ, Numan M, Schenk H, Weiss Z, Klika Z (1998) Clay Clay Miner 46:232–239
20. Breu J, Stoll A, Lange KG, Probst T (2001) Phys Chem Chem Phys 3:1232–1235
21. Mering J (1975) Smectites, chapter 4. In: Gieseking JE (ed) Soil components, vol 2, Inorganic components. Springer, Berlin Heidelberg New York, pp 97–119
22. Vahedi-Faridi A, Guggenheim S (1997) Clay Clay Miner 45:859–866
23. Vahedi-Faridi A, Guggenheim S (1999) Clay Clay Miner 47:338–347
24. Slade PG, Stone PA (1984) Clay Clay Miner 32:223–226
25. Cerius^2 documentation (June 2000) Molecular Simulations Inc, San Diego (CD-ROM)
26. Lehn JM (1990) Angew Chem Int Ed Engl 29:1304–1319
27. Nangia A, Desiraju GR (1998) Acta Crystallogr A 54:934–944
28. Gavezzotti A (1991) J Am Chem Soc 113:4622–4629
29. Dollase WA (1986) J Appl Crystallogr 19:267–272
30. Suortti P (1972) J Appl Crystallogr 5:325–330
31. Comba P, Hambley TW (1995) Molecular modeling of inorganic compounds. VCH, Weinheim, pp 5–52
32. Rappé AK, Casewit CJ, Colwell KS, Goddard WAIII, Skiff WM (1992) J Am Chem Soc 114:10024–10035
33. Dauber-Osguthorpe P, Roberts VA, Osguthorpe DJ, Wolff J, Genest M, Hagler AT (1988) Proteins: Struct, Funct, Genet 4:31–47
34. Clark M, Cramer RDIII, Van Opdenbosh N (1989) J Comput Chem 10:982–1012
35. Sun H (1994) J Comput Chem 15:752–768
36. Mayo SL, Olafson BD, Goddard WAIII (1990) J Phys Chem 94:8897–8909
37. Rappé AK, Goddard WAIII (1991) J Phys Chem 95:3358–3363
38. Ewald PP (1921) Ann Phys (Leipzig) 64:253–287
39. Karasawa N, Goddard WAIII (1989) J Phys Chem 93:7320–7327
40. Koudelka B, Čapková P (2002) J Mol Model 8:184–190
41. Erk P (1999) In: Braga D, Orpen G (eds) Crystal engineering: from molecules and crystals to materials. Kluwer, Dordrecht, The Netherlands, pp 143–161
42. Verwer P, Leusen FJJ (1998) Rev Comput Chem 12:327–365
43. Frenkel D, Smit B (1996) Understanding molecular simulation. Academic Press, San Diego, pp 19–88
44. Harris KDM, Kariuki BM, Johnston RL (2001). In: Kužel R, Hašek J (eds) Advances in structure analysis. Czech and Slovak Crystallographic Association, Prague, pp 190–204
45. Pospíšil M, Čapková P, Měřínská D, Maláč Z, Šimoník J (2001) J Colloid Interface Sci 236:127–131
46. Tzou MS, Pinnavaia TJ (1988) Catal Today 2:243–259
47. Yamanaka S, Hattori M (1988) Catal Today 2:261–270
48. Bartley GJJ (1988) Catal Today 2:233–241
49. Chen G, Han B, Yan H (1998) J Colloid Interface Sci 201:158–163
50. Tahani A, Karroua M, Van Damme H, Levitz P, Bergaya F (1999) J Colloid Interface Sci 216:242–249
51. Lee JF, Mortland MM, Chiou CT, Kile DE, Boyd SA (1990) Clay Clay Miner 38:113–120
52. Polverejan M, Liu Y, Pinnavaia TJ (2000) In: Sayari A (ed) Studies in surface science and catalysts 129. Elsevier, Amsterdam, pp 401–416
53. Okada A, Usuki A (1995) Mater Sci Eng C 3:109–115
54. Breu J, Raj N, Catlow CRA (1999) J Chem Soc Dalton Trans 6:835–845
55. Beall GW, Tsipursky SJ (1998) Proceedings of Additives 98, Orlando, Fla., pp 266–280
56. Boyd SA, Mortland MM, Chiou CT (1988) Soil Sci Soc Am J 52:652–657
57. Lee JF, Crum JR, Boyd SA (1989) Environ Sci Technol 23:1365–1372
58. Chattopadhyay S, Traina SJ (2000) J Colloid Interface Sci 225:307–316
59. Kibbey TCG, Hayes KF (1993) Environ Sci Technol 27:2168–2173
60. Lagaly G, Weiss A (1969) In: Heller L (ed) Proceedings of the international clay conference, Tokyo. Israel University Press, Jerusalem, pp 61–80
61. Hackett E, Manias E, Giannelis EP (1998) J Chem Phys 108:7410–7415
62. Čapková P, Burda JV, Weiss Z, Schenk H (1999) J Mol Model 5:8–16
63. Pospíšil M (2002) Complex structure analysis of intercalates using molecular simulations. Thesis, Charles University Prague
64. Endo T, Nakada N, Sato T, Shimada M (1988) J Phys Chem Solids 49:1423–1428
65. Estévez MJT, Arbeloa FL, Arbeloa TL, Arbeloa IL (1995) J Colloid Interface Sci 171:439–445
66. Estévez MJT, Arbeloa FL, Arbeloa TL, Arbeloa IL (1994) J Colloid Interface Sci 162:412–417
67. Chaudhuri R, Arbeloa FL, Arbeloa IL (2000) Langmuir 16:1285–1291
68. Arbeloa FL, Chaudhuri R, Arbeloa TL, Arbeloa IL (2002) J Colloid Interface Sci 246:281–287
69. Pospíšil M, Čapková P, Weiss Z, Maláč Z, Šimoník J (2002) J Colloid Interface Sci 245:126–132